KSCE Journal of Civil Engineering (2017) 21(7):2908-2918
DOI 10.1007/s12205-017-0989-8

Tunnel Engineering
pISSN 1226-7988, eISSN 1976-3808
www.springer.com/12205

Surface Settlement Prediction for EPB Shield Tunneling in Sandy Ground

Yong Fang*, Chuan He, Ali Nazem***, Zhigang Yao****, and Jacob Grasmick*****

Received November 24, 2015/Revised October 16, 2016/Accepted December 13, 2016/Published Online February 17, 2017

Abstract

Ground volume loss induced by shield tunnel construction is the major factor leading to ground settlement and deformation. The general equations predicting surface settlement based on ground volume loss involve a settlement trough width coefficient (parameter *i*) which in previous models was set as a constant in both the transverse and longitudinal directions. In this work, the equations predicting surface settlement during the construction were modified by introducing the parameter *j* – the width coefficient in the longitudinal direction, assumed to be different from that in the transverse direction. A model shield machine was adopted to carry a laboratory test under 1 *g* to investigate surface settlement induced by earth-pressure-balance shield tunnel construction in unsaturated sandy soil. The surface settlement during the excavating observed in the test was compared with that predicted by general equations from previous studies and the modified. The results showed that surface settlement above shield machine obtained by the modified equation proposed here fits the test data better than those obtained by the general equations because of the introduced longitudinal width coefficient.

Keywords: *shield tunneling, settlement, ground volume loss, longitudinal width coefficient, physical model test*

1. Introduction

Ground settlement (surface vertical movement) is a critical concern to both the surface (Melis *et al.*, 2002; Papastamos *et al*., 2014) and subsurface facilities (Vorster *et al*., 2005), particularly in urban settings (Liao *et al*., 2009). Many metro tunnels are being constructed using Earth Pressure Balance shield machine (EPB) which has many advantages. During EPB shield driving, ground settlement often needs to be controlled to minimize possible damage to adjacent buildings and infrastructures. Therefore, tunnel engineers and designers must evaluate the magnitude and distribution of the settlement in both the transverse and longitudinal directions.

Field testing is an important method for investigating ground displacement caused by shield (Mathew and Lehane, 2012). Previous studies have yielded valuable data from field measurements in various soil conditions. Based on a large number of field data, Peck (1969) developed the concept of ground loss and deduced important characteristics to fit the surface settlement profile in the transverse direction using a Gaussian curve, with the maximum settlement S_{max} and settlement trough width coefficient *i*, which is the horizontal distance to the inflexion point. Peck and other authors have considerably improved the formula, specifically with regard to the estimation of the parameter *i* in various conditions. For example, Clough and Schmidt (1981) presented *i* as a function of the diameter and buried depth of the tunnel; O'reilly and New (1982) demonstrated the linear relation between *i* and the buried depth in a simple layer; Attewell and Hurrell (1985) showed that *i* is related to soil characteristics as well as to construction factors. In drained soils such as sand or gravel the Gaussian curve, however, does not always fit the settlement trough data (Celestino *et al.*, 2000). In this case, Sugiyama *et al.* (1999) suggested that the published *i* values can be modified to fit the trough shape.

Ground settlement caused by shield tunneling was also investigated analytically. Sagaseta (1987, 1988) gave a solution for the stress field induced by near-surface ground loss and proposed the parameter of ground volume loss to predict surface subsidence in homogeneous and incompressible soil. Verruijt and Booker (1996) andPark (2005) developed an analytical method to find the solution of surface settlement caused by tunneling. Although the analytical method has several advantages in addressing the ground surface settlement issue (Nazem *et al*., 2015); there are major constraints in application. For instance, there are many simplifications such as a plain strain assumption

*Professor, Key Laboratory of Transportation Tunnel Engineering, Ministry of Education, Southwest Jiaotong University, Chengdu 610031, China (Corresponding Author, E-mail: fy980220@swjtu.cn)
**Professor, Key Laboratory of Transportation Tunnel Engineering, Ministry of Education, Southwest Jiaotong University, Chengdu 610031, China (E-mail: Chuanhe21@163.com)
***Ph.D. Student, Civil and Environmental Engineering, Colorado School of Mines, Golden CO 80401, US (E-mail: anazem@mymail.mines.edu)
****Graduated Student, Key Laboratory of Transportation Tunnel Engineering, Ministry of Education, Southwest Jiaotong University, Chengdu 610031, China (E-mail: 1916749996@qq.com)
*****Ph.D. Student, Civil and Environmental Engineering, Colorado School of Mines, Golden CO 80401, US (E-mail: jgrasmic@mines.edu)

(Chou and Bobet, 2002), elastic behavior (Park, 2004), and soil isotropy. Loganathan *et al.* (2000) and Franzius *et al*. (2005) suggested that the actual gap around the shield is oval because of the sinking of the segment lining, the three-dimensional elastic-plastic movement of the cutting face soil, and the tilting of the shield machine. While in a sandy layer, because of the discontinuity in ground deformation, the theoretical formula does not fit the settlement trough data well.

When analyzing field data, it is difficult to identify the effect of individual factors such as geology, construction method, and measurement errors. A centrifuge test can reproduce the full-scale ground behavior within a small-scale model. It has provided many useful data related to shield tunneling in test soils (Nomoto *et al*., 1999; Loganathan *et al*., 2000; Marshall and Mair, 2011). These studies demonstrated that the settlement trough profile was similar to the Gaussian curve. Bolton *et al.* (1996) developed a method to simulate shield tunnel construction using drum centrifuge tests. They obtained good simulations of the settlement trough, but the tail void formation process was ignored in their model. Marshall *et al.* (2012) examined the effect of tunnel size, depth, and volume loss in sandy ground using a centrifuge test. However, it is difficult to accurately model the construction process of a shield tunnel using a centrifuge test because of instrument limitations. Moreover, no information about the longitudinal settlement was presented.

Physical model tests under 1 *g* are another method of investigating the settlement caused by shield tunneling. Kim (1996) performed scaled model tests under 1 *g* to examine the interaction between closely spaced tunnels in clay and reported that the additional complexities of using a centrifuge outweighed the possible advantages. Other authors used physical model tests under 1 *g* to investigate ground movement caused by the construction of shield tunnels (Zhu *et al*., 2006; Chapman *et al.*, 2007). However, these tests focused on the interaction between the shield machine and the ground. Construction processes such as segment placement, grouting, etc. were ignored. He *et al.* (2012) obtained the process of surface settlement induced by the construction of twin tunnels using a laboratory model test of shield driving.

This paper focuses on studying the prediction of surface settlement caused by shield tunneling. In the formulas proposed by Peck (1969) and other investigators, the trough width coefficient parameter *i*, which represents the inflection point of the settlement trough, is an important parameter for predicting the surface settlement. Parameter *i* was also considered to be constant in both transversal and longitudinal direction in the estimation of longitudinal surface settlement (Attewell and Woodman's (1982)). In this work, the longitudinal trough width coefficient parameter *j*, assumed to be different from that in the transverse direction, was put forward to develop equations proposed by Attewell and Woodman (1982) and Liu and Hou (1991). In addition, an Φ = 52 mm model shield machine was employed to carry out indoor tests under 1 *g* gravity field to investigate surface settlement induced by earth-pressure-balance shield tunnel construction in unsaturated sandy soil. The surface settlement during the excavating observed in the test was compared with that predicted by general equations from previous studies and the modified.

2. Recapitulation of Settlement Prediction Models

Empirical methods are based on the observation of field data during tunnel excavation. Peck (1969) considered that the volume of the settlement trough in the transverse direction is equal to the ground volume loss induced by the shield tunneling in undrained soil. Peck and other researchers (Schmidt, 1969; O'reilly and New, 1982; Mair *et al*., 1993; Lee *et al*., 1999; Chen *et al*., 2011) demonstrated a good fit between the Gaussian distribution curve and the surface settlement in transverse. The curve has two important parameters: the volume loss parameter V_l which is equal to the volume of the settlement trough per meter, and the trough width coefficient i (Fig. 1). The surface settlement at point x is generally expressed as

$$S(x) = \frac{V_l}{\sqrt{2\pi}\cdot i}\exp(-x^2/2i^2) \tag{1}$$

These methods were generally used in estimating ground settlement in a transverse direction when the shield tunneling is finished while the settlement acquired in the longitudinal direction is ignored. Nomoto *et al.* (1999) proposed that the longitudinal settlement at point y above the tunnel central line can be described as the function of the tail void thickness v:

$$S(y)/v = ay + by^2 + cy \tag{2}$$

where a, b, and c are coefficients related to the construction and soil conditions. Based on field work, Attewell and Woodman (1982) proposed a cumulative error function to depict the surface settlement along the tunnel axis. The settlement at point (x, y) can be described as

$$S(x,y) = \frac{V_l}{\sqrt{2\pi}i}\exp\frac{-x^2}{2i^2}\left[\varnothing\left(\frac{y-y_i}{i}\right)\varnothing\left(\frac{y-y_f}{i}\right)\right] \tag{3}$$

where V_l and i are the same as in Peck's equation, y_f and y_i denote the location of the cutting head at the start and end of the shield driving, respectively, and Ø(a) is the normal function where Φ(0) = 0.5 and Φ(∞) = 1. Attewell and Woodman assumed that the ground volume loss forms in the cutting face. Thus, this approach

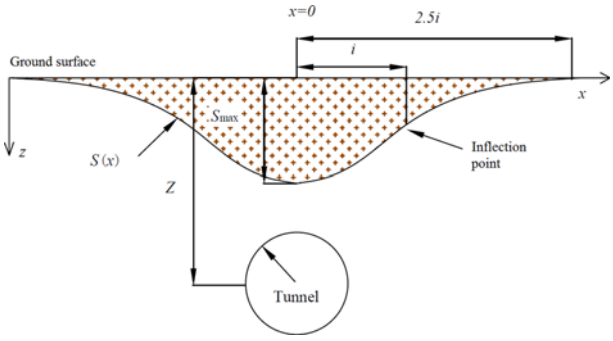

Fig. 1. Transverse Settlement Trough

works well in open-faced tunnel construction. In close-faced tunnel construction, there is significant face support; therefore, the majority of volume loss is associated with the tail void (Grasmick *et al.*, 2015; Mooney *et al.*, 2015). Liu and Hou (1991) modified Attewell and Woodman's (1982) formula by dividing the volume loss into the loss at the cutting face and the loss at the shield tail. The longitudinal surface settlement at point y above the tunnel central line was modified by Liu and Hou (1991) as

$$S(y)=\frac{V_{lh}}{\sqrt{2\pi}i}\left[\varnothing\left(\frac{y-y_i}{i}\right)-\varnothing\left(\frac{y-y_f}{i}\right)\right]+\frac{V_{ll}}{\sqrt{2\pi}i}\left[\varnothing\left(\frac{y-y_i'}{i}\right)-\varnothing\left(\frac{y-y_f'}{i}\right)\right] \quad (4)$$

where V_{lh} and V_{ll} are the volume loss that forms in the cutting face and shield tail, respectively; y_f, y_i and y_f', y_i' are the locations of the cutting head and shield tail at the beginning and end of the driving, respectively.

The ground volume loss comes into being with the driving of shield machine. In the longitudinal direction, the ground loss distribution is obviously different from that in transverse, as it occurs along a wider span, from in front of the cutting face to behind the shield tail. Fig. 2 shows the longitudinal settlement curves induced by shield machines with different lengths. In the same conditions of ground volume loss, cover depth, geology and transverse dimensions, the longitudinal settlement curve caused by shield machine A is steeper than that caused by shield machine B which has a bigger length (Fang *et al.*, 2015). Therefore, the equation proposed by Attewell and Woodman (1982) needed to be modified by introducing the parameter j as

$$S(x,y)=\frac{V_l}{\sqrt{2\pi}i}\exp\frac{-x^2}{2i^2}\left[\varnothing\left(\frac{y-y_i}{j}\right)-\varnothing\left(\frac{y-y_f}{j}\right)\right] \quad (5)$$

where parameter j is equivalent to the distance between the two inflection points of the longitudinal settlement curve and also represents the steepness of longitudinal surface settlement as shown in Fig. 2. Considering that the ground volume loss forms along the shield, from the cutting head to the shield tail, y_f and y_i are the locations of the middle length of shield machine at the start and end of the driving. Likewise, the equation developped by Liu and Hou (1991) can be rewritten as

$$S(y)=\frac{V_{lh}}{\sqrt{2\pi}i}\left[\varnothing\left(\frac{y-y_i}{j}\right)-\varnothing\left(\frac{y-y_f}{j}\right)\right]+\frac{V_{ll}}{\sqrt{2\pi}i}\left[\varnothing\left(\frac{y-y_i'}{j}\right)-\varnothing\left(\frac{y-y_f'}{j}\right)\right] \quad (6)$$

When longitudinal distribution of ground volume loss is affected mainly by the length of the shield machine, the parameter j has a simple relation to the parameter i, for example

$$j=i(L-D_s)/2 \quad (7)$$

where L and D_s is the length and out- diameter of the shield machine respectively.

3. The Scaled Model Test Setup and Procedure

3.1 Summary of Model Machine

A scaled EPB model shield machine was used to carry out the

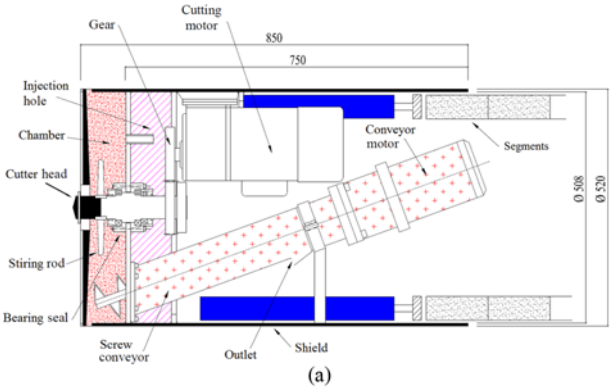

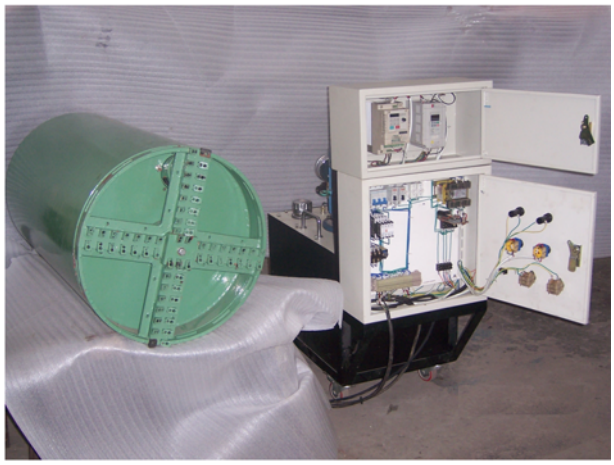

Fig. 3. Model Shield Machine (unit: cm): (a) Dimensions, (b) Control Panel

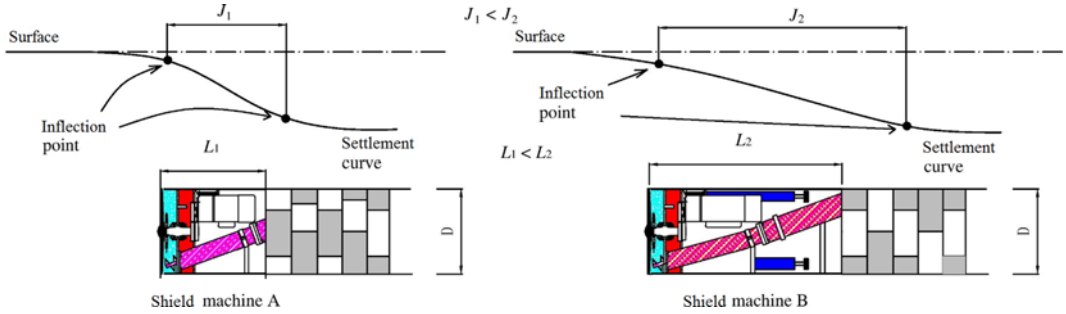

Fig. 2. Longitudinal Settlement Distribution Above Tunnel

laboratory test. It consists of a steel shell, advancing sets, cutting sets and discharging sets as shown Fig. 3. The shield has the dimensions: length, 850 mm; outer diameter, 520 mm; and thickness, 6 mm. The advancing sets comprise of four hydraulic cylinders fixed inside the model shield machine at equal spacing to provide the advancing thrust. All the cylinders can exert a maximum total thrust of 20 kN. The extension velocity and thrust magnitude of each cylinder is the same and can be adjusted via the control box. The cutting sets include a cutter head, a motor and the related bearing, seal and gears. The cutter head with an opening ratio of 54.5% composed of spokes and cutters and is driven by an electric motor with a maximum torque of 500 N·m. The rotation speed of the cutter head can be changed continuously up to 9 rpm both in clockwise and counterclockwise directions by the control box. The discharging sets include a screw conveyor (outer diameter: 80 mm) and an electric motor. The conveyor is driven by the motor which can provide a maximum torque of 50 N·m and continuous rotation speed up to 20 rpm. During the test, the chamber is filled with the excavated soil while the screw conveyor driven by the conveyor motor rotates and discharges the soil. During the excavation by the EPB shield machine, control of the chamber pressure improves the stability of the cutting face and minimizes the volume loss and ground displacement (Merritt and Mair, 2006; Peila *et al*., 2007; Merritt and Mair, 2008; Peila *et al*., 2013). If the volume of soil discharged from the screw conveyor is more than the volume of soil excavated by the cutter head, the ground volume loss in the cutting face increases significantly. Hence, the volume of soil discharged is generally expected to be equal to that excavated.

After the model shield machine has moved forward a certain distance, the wood segments are assembled manually in the tail of the shield. The segments have a 500 mm outer diameter, 50 mm thickness and 50 mm width. Four segments were joined to form a ring by eight annular pin bolts which are equally distributed with a central angle of 45°, as shown in Fig. 4. The installation sequence was segment B, D, A, and C. The assembled segment rings were connected to form the lining structure by eight longitudinal pin bolts. Furthermore, to increase the stiffness of segment rings and prevent excessive deformation which causes unexpected ground volume loss, a Φ10-mm steel ring bar was fixed tightly onto the inner face for each ring. A photo of the assembled segment rings is shown in Fig. 5.

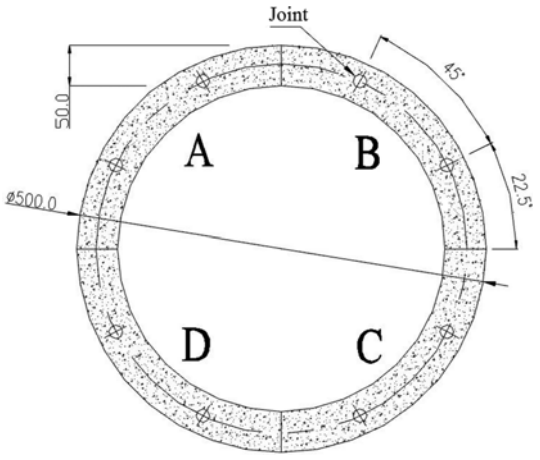

Fig. 4. Model Segments Ring

Fig. 5. Driving of Model Shield Machine

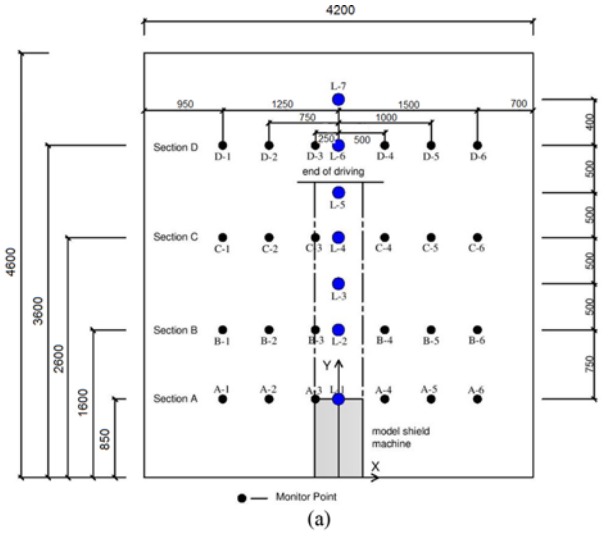

(a)

(b)

Fig. 5. Driving of Model Shield Machine

3.2 Test Preparation

The driving of the model shield machine was carried out in a tank which has the dimensions as follows: length, 460 cm; width, 420 cm and height, 180 cm. The cover depth of the tunnel was set to be 66 cm and the distance from tunnel center to the surface was 91 cm (C/D is 2.64). Fig. 6 shows the coordinate system and layout of the monitoring points on the surface. The settlement at each point was measured by displacement sensor which has a range of 5 cm and an accuracy of ±0.01 mm.

The tank was filled with sandy soil taken from the construction site of the Cheng-Guan station of the Chengdu Metro line 2, China. The target stratum of Quaternary Holocene alluvium (Q_4^{al}) was at a depth of 8 m. The grain size composition and material parameters suggested by the site investigation reports are shown in Table 1 and Table 2. The sandy soil obtained from the construction site was compacted in the laboratory until the density of the test soil was equal to that in Table 2. In addition, the model shield machine was buried in the ground beforehand while the initial stage where the shield machine started from the shaft was ignored.

Soil conditioning is generally necessary for an EPB shield machine to excavate in sandy stratum. A number of publications (Peila *et al*., 2007; Vinai *et al*., 2008; Gharahbagh *et al*., 2014) showed that soil conditioning assists the excavation work by enhancing the flowability and impermeability of the excavated soil, transmitting the pressure in the chamber and along the screw conveyor, reducing frictional forces and abrasive wear. In practice, foam and bentonite slurry are widely adopted in the soil conditioning of EPB shield construction. In this test, bentonite slurry was pumped into the chamber through the injection hole at a 1:5 ratio of slurry volume to excavation soil volume.

Table 1. Grain Size Composition

Grain size	2 mm~ 0.5 mm	0.5 mm~ 0.25 mm	0.25 mm~ 0.075 mm	<0.075 mm
Percent(%)	7	78	10.5	4.5

Table 2. Natural Material Parameters

Density (g/cm^3)	Deformation modulus (MPa)	Lateral pressure coefficient	Cohesion (kPa)	Friction angle (°)	Moisture content (%)
18.5	5.0	0.35	1.5	28	8

Table 3. Ground Volume Loss at the Cutting Face

Part	I	II	III	IV
Face location (cm)	85–160	160–210	210–260	260–320
Theoretical excavated volume (m^3)	0.16671	0.11114	0.11114	0.13337
Actual exhausted volume (m^3)	0.16571	0.11017	0.10976	0.13182
Ground volume loss (m^3/m)	0.00133	0.00129	0.00184	0.00207

Back fill grouting can prevent ground movement and ensure the stability of the segment rings in the early stages of excavation. In the test, each segment has a grouting hole. After the model shield machine finished the advancing, grouting was carried out behind the previous segments. A mix of 1:1 hydrated to water was pumped into the void between the segment ring and test ground. As the mixture is hard to penetrate the ground, the volume of hydrated plaster injected is usually less than that of the tail void. The grouting volume was recorded as an important parameter for the estimation of ground volume loss in the tail.

3.3 Testing Results and Discussion

3.3.1 Ground Volume Loss

The model shield driving process was divided into four parts along the driving direction as shown in Fig. 7. The ground volume loss at the cutting face and the tail of the model shield machine were measured separately for each part. The ground

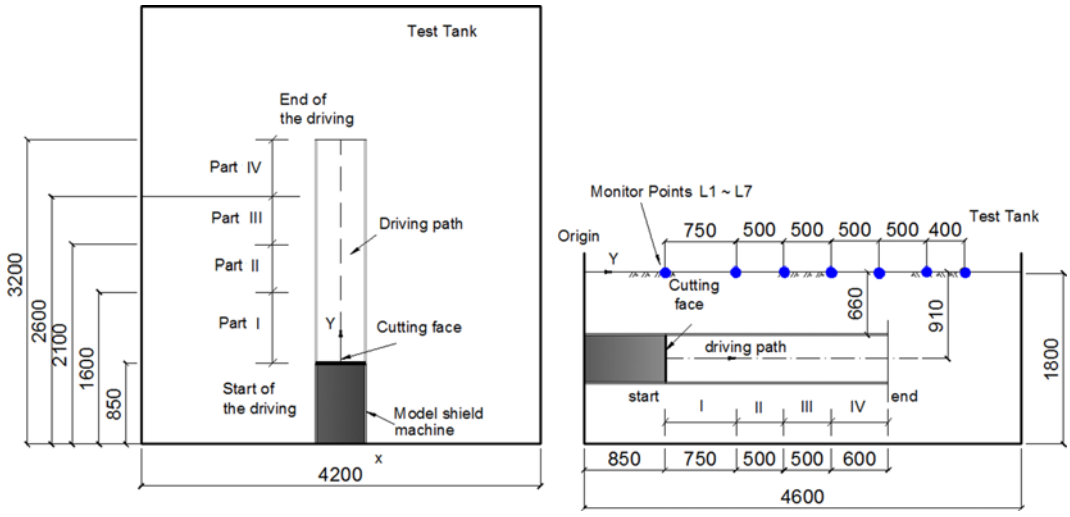

Fig. 7. Excavation Scheme (unit: mm)

Table 4. Ground Volume Loss at the Shield Tail

Part	I	II	III	IV
Tail location (cm)	0-75	75-125	125-175	175-235
Volume of tail void (m^3)	0.01202	0.00801	0.00801	0.00961
Volume of grouting (m^3)	0.01001	0.00606	0.00615	0.00788
Ground volume loss (m^3/m)	0.00267	0.0026	0.00248	0.0023

volume loss at the face V_{lh} is given by subtracting the theoretical soil volume and the injection weight of bentonite slurry from the volume that was actually removed.

$$V_{lh} = \frac{W_d - W_b}{\gamma_s} - V_{th} \tag{8}$$

Where W_d is the weight of discharged soil, W_b is the weight of bentonite slurry injected and γ_s is the unit weight of the model soil before excavated. V_{th} is the theoretical excavated volume, which is calculated from the outer diameter of the model shield machine and the driving distance. The ground volume loss at the cutting face is shown in Table 3.

The ground volume loss at the shield tail V_{lt} is equal to the void volume V_v between the segment and the ground, minus the volume of the grouting V_{gr} in the tail.

$$V_{lt} = V_v - V_{gr} \tag{9}$$

The void volume V_v is calculated using the outer diameter (52 cm) of the shield tail, the outer diameter (50 cm) of the segment ring, and the driving distance. The V_{gr} is the volume of injected plaster. The ground volume loss at the shield tail is shown in Table 4. The total ground volume loss V_l is

$$V_l = V_{lh} + V_{lt} \tag{10}$$

According to Table 3 and Table 4, the average ground volume loss per meter throughout the whole shield driving process is V_l = 0.00414 m^3/m and the average ground volume loss ratio can be calculated to be 1.95% by Eq, (11).

$$\varepsilon = 4V_l / \pi D^2 \tag{11}$$

where D is the outer diameter of the segment rings.

3.3.2 Width Coefficient of Settlement Trough

Many literatures about the trough width coefficient i have been published. Peck (1969) suggested Eq. (12) for the excavation of sandy soil. Schmidt (1969) suggested Eq. (13) for the excavation of soft ground by shield machines. O'reilly and New (1982) suggested Eq. (14) for the excavation of all the types of soils by shield machines.

$$i_1 = Z / \left(\sqrt{2\pi} \tan\left(45 - \frac{\phi}{2} \right) \right) \tag{12}$$

$$i_2 = (D/2) \times (Z/D)^{0.8} \tag{13}$$

$$i_3 = kZ \tag{14}$$

where Z is the depth to the tunnel axis, D is the tunnel diameter, k is the coefficient of trough width and Ø Is the internal friction angle of the ground. Teng and Zhang (2012) suggested k to be 0.5 for the EPB shield driving in sandy cobble ground by finite element method and particle flow code (PFC^{2D}). In this paper the average of these methods was used to estimate the standard deviation, i, value (Chakeri *et al.*, 2013).

$$i = (i_1 + i_2 + i_3)/3 \tag{15}$$

In the test Z is 0.91 m, D is 0.5m and φ is 28°. Inserting the relevant values into Eq. (12)~Eq. (15), the transverse width coefficient of the settlement groove was calculated as i = 0.58 m. The length of the model shield machine is L = 0.85 m and the outer diameter is D_s = 0.52 m. Using these values and Eq. (7), the longitudinal width coefficient can be calculated as j = 0.745 m. In some practical engineering cases, the length of the shield machine is approximately equal to its width, so the width coefficient in the transverse direction is almost the same as that in the longitudinal direction. In other cases, such as the mini-type shield machine, the length of the machine is generally bigger than the width, and the width coefficients in longitudinal direction is bigger than that in transverse.

3.3.3 Transversal Surface Settlement

Figure 8 shows the surface settlement for all sections when the cutting face located at Y = 160 cm, 210 cm, 260 cm and 320 cm. It can be seen that the settlement troughs of all sections have the similar shape and the maximum settlement in all sections locate above the central line of the tunnel. Because of the driving direction of model shield machine, section A has the maximum surface settlement, then section B and section C, and section D has the minimum surface settlement. At point L-1(section A), settlement increases to -2.07 mm, -2.56 mm, -2.84 mm and -3.01 mm when the model shield machine driving from Y = 85 cm (face location at the start of the driving) to Y = 160 cm, Y = 210 cm, 260 cm and 320 cm (face location at the end of the driving). When the cutting face located at Y = 210 cm, where the shield tail had passed section A about 40 cm, the settlement of point L-1 account for 85% of the maximum settlement. It can be seen in Fig. 8(a) that the settlement behind the shield tail account for small part of the maximum settlement. Section B experiences the full process of the closing, passing and departing of the model shield machine during the driving test. The settlement of point L-2 (section B) increases to -0.98 mm, which account for 34.3% of the maximum settlement at this point, when the cutting face moving from Y = 85 cm to the location beneath section B (Y = 160 cm). When shield tail passed section B about 15 cm, the settlement of point L-2 increased to -2.45 mm, which account for 85.7% of the maximum settlement. It is shown in Fig. 8(a) and Fig. 8(b) that most of the surface settlement comes into being during the passing of shield machine. The settlement of point L-4 (section C) is -0.94 mm when the cutting face arriving at Y = 260 cm (beneath section C), and increases to -1.91 mm at the end of the driving, where the cutting face locates at Y = 320 mm and point L-4 still locates above the shield machine. Fig. 8(c) and Fig. 8(d) also shows that the settlement before the

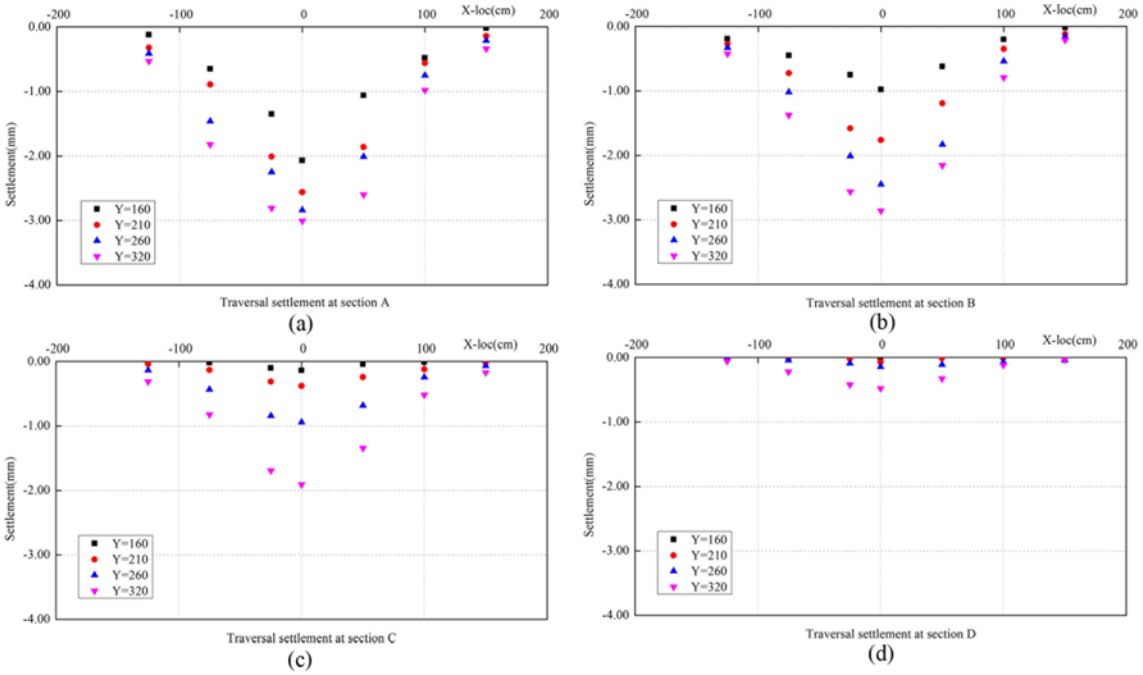

Fig. 8. Surface Settlement at: (a) Section A, (b) Section B, (c) Section C, (d) Section D

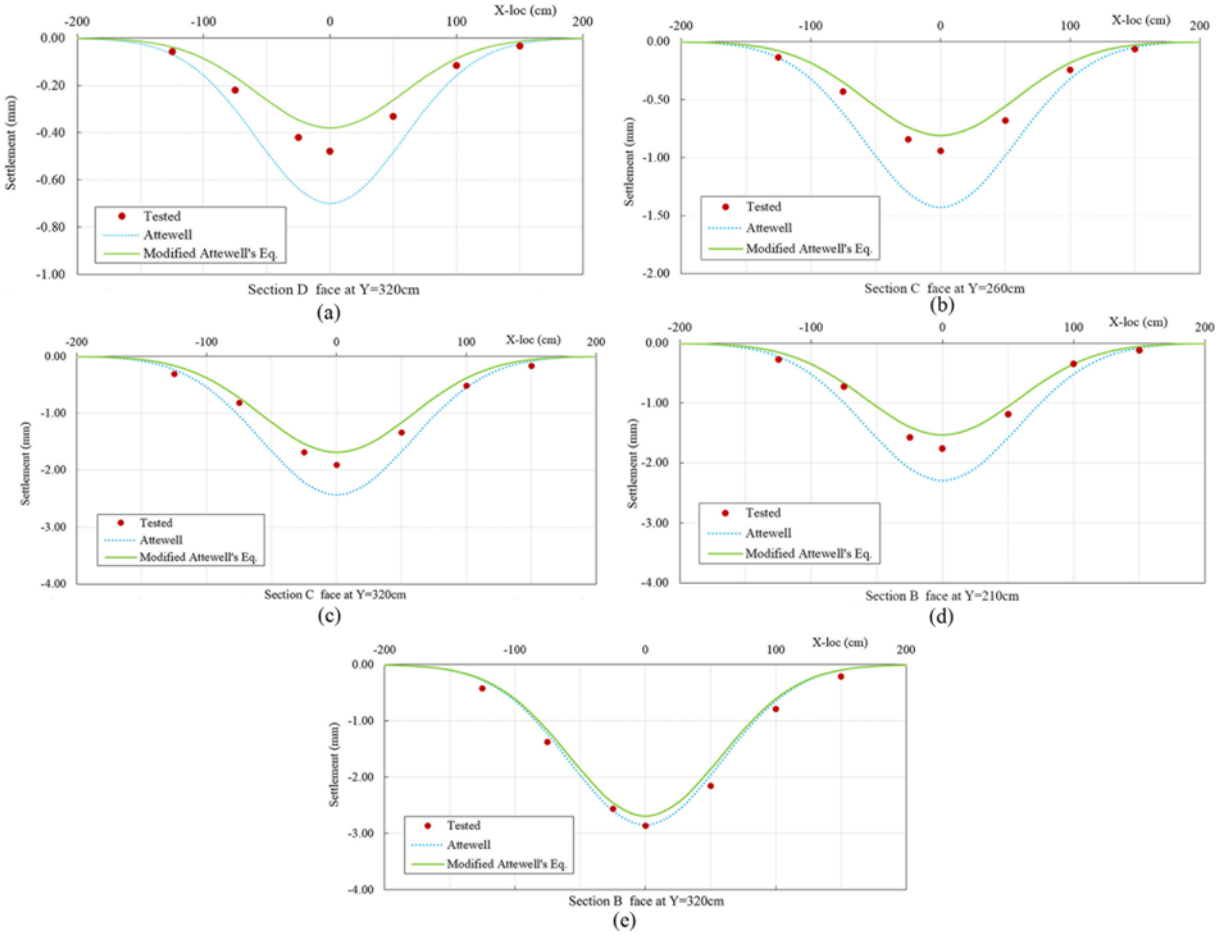

Fig. 9. The Comparison of Surface Settlement between the Tested and Predicted Value: (a) Ahead of the Cutter Head, (b) Above the Cutter Head, (c) Above the Shield Body, (d) Above the Shield Tail, (e) Behind the Shield Tail

arriving of the cutting face account for small part of maximum settlement.

In this paper, five cases of the transversal surface settlement were compared between the tested and predicted data as shown in Fig. 9. When Section D is 4 cm ahead of the cutterhead, the maximum surface settlement was 0.48 mm while it was estimated to be 0.70 mm by Eq. (3) and 0.38 mm by Eq. (5). Fig. 9(a) shows that the prediction of Eq. (5) is closer to the tested value than that of Eq. (3). The difference of the predictions for the maximum settlement by Eq. (5) and Eq. (3) is 20.8% and 45.8% respectively. It can be seen that the two transversal surface settlement troughs are similar as Eq. (3) and Eq. (5) have the same transversal width coefficient i although the maximum of the surface settlement was different.

When Section C was directly above the cutterhead, the maximum surface settlement was 0.94 mm while it was estimated to be 1.43 mm by Eq. (3) and 0.81 mm by Eq. (5). The predicted settlement trough of Eq. (5) is also closer to the tested value than that of Eq. (3). The difference of the predictions for the maximum settlement by Eq. (5) and Eq. (3) is 13.8% and 52.1% respectively. Fig. 9(b) also shows that the difference between the prediction of Eq. (3) and the tested value reached the maximum when the cutting head beneath the monitor section. Section C (Y = 260 cm) was above the tail of the shield when the cutting head located at Y = 320 and the maximum surface settlement was tested to be 1.91mm while it was estimated to be 2.43 mm by Eq. (3) and 1.69 mm by Eq. (5). The tested surface settlement in section C also fell in between the settlement troughs predicted by Eq. (3) and Eq. (5) as shown in Fig. 9(c).

Section B (Y = 160 cm) was also above the tail of the shield machine when the cutting head located at Y = 210 cm and the maximum surface settlement was tested to be 1.58 mm. Fig. 9(d) shows that the settlement troughs tested and predicted by Eq. (3) and Eq. (5) of this case are all similar to those of the section C (Y = 260 cm) with the cutting head location Y = 320 cm. It can be concluded that the surface settlement depends on the locations relative to the shield machine when the ground volume loss is constant. When the cutting head located at Y = 320 cm, the shield tail had passed Section B for 75cm (about 1 j) and the maximum surface settlement was tested to be 2.56 mm. It is shown in Fig. 9(e) that the predicted settlement troughs of Eq. (3) and Eq. (5) are very close although they are both a little smaller than the tested value. The difference between the prediction of the maximum settlement by Eq. (3) and Eq. (5) is 5.6%. Hence, the Eq. (3) and Eq. (5) have the same results for the predictions of the surface settlement that the shield tail passed for more than 1 j.

3.3.4 Longitudinal Surface Settlement

Using the relevant parameter values in Eq. (3)~Eq. (5), the surface settlement was predicted and compared with the results of model test. Fig. 10 shows that the shapes of the three sets of resulting curves are clearly different. When the cutting face is located at y = 160 cm (Fig. 10(a)), the surface settlement above shield machine at point L-1 (y = 85 cm) and L-2 (y = 160 cm) was tested to be -2.07 mm and -0.98 mm respectively. The settlement at point L-1 and L-2 predicted by Eq. (3) (Attewell and Woodman, 1982) is -2.56 mm and -1.43 mm, and the difference to the tested value is 24% and 46% respectively. The settlement at the same point predicted by Eq. (4) (Liu and Hou, 1991) is smaller than the tested value and the difference is 15% at L-1 and 30% at L-2. The predicted settlement by Eq. (5) (modified Attewell and Woodman's (1982) method) at L-1 and L-2 is -1.9 mm and -0.81 mm, and the difference to the tested value is 8% and 17% respectively.

The ground settlement increased as the model shield machine

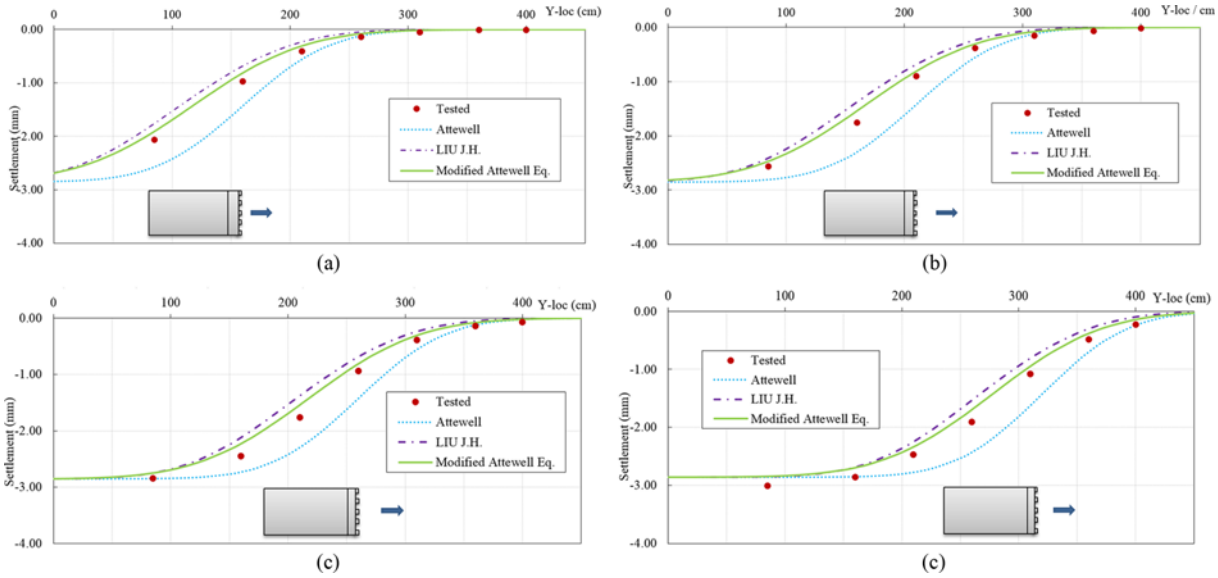

Fig. 10. longitudinal Surface Settlement Along the Central Line (monitor point L1~L7): (a) Face at Y = 160 cm, (b) Face at Y = 210 cm, (c) Face at Y = 260 cm, (d) Face at Y = 320 cm

moved forward in part II. When the cutting face was at $y = 210$ cm, the shapes of the three simulated curves are similar to those in Fig. 10(b). Surface settlement at point L-1 ($y = 85$ cm) which located 45 cm (0.9D) behind the shield tail was tested to be -2.56 mm. The predicted value at L-1 by Eq. (3), Eq. (4) and Eq. (5) is -2.81 mm, -2.40 mm and -2.46 mm, and the difference to the tested value is 10%, 6% and 4% respectively. At point L-2 (y = 160 cm) and L-3 (y = 210 cm) which locates above the model shield machine, the tested settlement is -1.76 mm and -0.91 mm respectively. The settlement predicted by Eq. (3) at the same point is -2.3 mm and -1.43 mm which is larger than the tested value and the difference is 31% and 57% respectively. The predicted value at these two point by Eq. (4) and Eq. (5) are smaller than the tested value. The settlement predicted by Eq. (5) is -1.54 mm at L-2 and -0.82 mm at L-3, which is closest to the test values, and the difference is 13% and 10%. Hence, as for the prediction of surface settlement above shield machine, Eq. (5) is the closest to the tested value, Eq. (3) has the maximum value which is larger than the tested one and Eq. (4) has the minimum value which is smaller than the tested one.

The ground settlement continued when the machine was driving through part III and part IV, and the shape of the longitudinal settlement distribution above the tunnel is similar to that in Part I and part II. The ground settlement curves obtained by the various models are compared in Fig. 10(c) and Fig. 10(d). At point L-3 (y = 210 cm), L-4(y = 260 cm) and L-5 (y = 310 cm), which are all above shield machine, the predicted settlement by Eq. (5) is still the closest to the tested value compared to that by Eq. (4) and Eq. (5). When the cutting face was at y = 260 cm, point L-1 ($y = 85$ cm) located 90 cm (1.8D) behind the shield tail. The tested settlement at L-1 was -2.84 mm. The predicted value at the same point by Eq. (3), Eq. (4) and Eq. (5) is -2.85 mm, -2.74 mm and -2.74 mm, and the difference to the tested value is 0.4%, 3.5% and 3.5% respectively. It can be seen that the predicted surface settlement of different methods are closer at the behind of the shield machine than above the shield machine. When the cutting face was at $y = 320$ cm, point L-1 ($y = 85$ cm) located 160 cm (3.2D) behind the shield tail. The tested settlement at L-1 was -3.01 mm. The predicted settlement at the same point by Eq. (3), Eq. (4) and Eq. (5) has the same value -2.85 mm, and the difference is 5.3%. Hence, the predicted surface settlement of different methods are the same at far behind of the shield machine. However, the maximum surface settlements predicted by all of the methods are smaller than the test values. The factors causing the difference include the ground solidification, segment deformation and other processes that occur after the shield machine passes. These factors also induce the ground movement and they are not included in all of the prediction models.

Generally, the Eq. (3) proposed by Attewell and Woodman (1982) and Eq. (5) that is modified by introducing the parameter j in this paper can both be used to predict the surface settlement during the driving of shield machine. These two equations are different in the estimation of the surface settlement due to the introduction of parameter j in the Eq. (5). Attewell and Woodman assumed that the ground volume loss forms in the cutting face. Thus, Eq. (3) works well in open-faced tunnel construction. Eq. (5) assumes that the ground volume loss comes into being near the middle length of shield machine. Thus Eq. (5) is more suitable in close-faced tunnel construction, where the majority of volume loss is associated with not only the cutting face but also the tail void (Grasmick *et al.*, 2015; Mooney *et al*., 2015). Hence, the surface settlement at any point estimated by Eq. (3) forms earlier than that estimated by Eq. (5) during the shield driving. On the other hand, if the length (L) of the machine is about equal to the diameter of the shield (D), the trough width coefficient in transverse direction is equal to that in longitudinal direction. However, if the length (L) of the machine is much bigger than the diameter (D) of the shield, the trough width coefficient in longitudinal direction is underestimated in Eq. (3). The transversal surface settlement at any point estimated by Eq. (3) is usually greater than that estimated by Eq. (5). However, the final surface settlement predicted by Eq. (3) and Eq. (5) are same. In Liu's model (Eq. (4)), the ground volume loss is assumed to form both in the cutting face and in the tail of the shield machine. The actual longitudinal trough is composed by the trough that caused by the ground volume loss in the cutting face and the trough that caused by the ground volume loss in the shield tail. Hence, the longitudinal settlement trough looks gentler and the trough width coefficient in longitudinal direction is overestimated. In this model (Eq. (5)), the difference of the dimensions between the longitudinal direction and transverse direction was represented by parameter j. The longitudinal settlement trough predicted by this model looks more reasonable than those predicted by Attewell's model and Liu's model.

4. Conclusions

Considering that the ground volume loss distribution in the transverse and longitudinal directions is different during the shield tunnel driving, the longitudinal settlement width coefficient j was introduced in this paper and the formula of predicting the surface settlement put forward by the Attewell and Woodman (1982) and Liu and Hou (1991) were modified. Laboratory model shield driving test was carried out to verify the validity of the longitudinal settlement width coefficient and the accuracy of the prediction model. The results show that the improved model can be used to estimate the surface settlement during the shield driving on the basis of known ground volume loss. The conclusions can be drawn as follows:

1. As for the prediction of surface settlement above shield machine during the excavation, Attwell and Woodman's (1982) method has the maximum predicted surface settlement, Liu and Hou's (1991) method has minimum predicted surface settlement and the modified Attewell and Woodman's method has the closest value to the tested one.
2. As for the prediction of surface settlement far behind the shield machine, the predicted surface settlements of different

methods are the same although they are smaller than the test values. The factors causing the difference include the ground solidification, segment deformation and so on. These factors induce the ground movement while they are not included in all the prediction methods.

3. From the view on the shape of longitudinal surface settlement curve, surface settlement predicted using the modified Attewell and Woodman's method has gentler inclines than that predicted using Attewell &Woodman's model because of the introduction of the longitudinal width coefficient *j*.

Acknowledgements

This paper was supported by the National Natural Science Foundation of China (No: 51278422, 51578460), the National Key Research and Development Program of China (2016YFC0802201).

References

Attewell, P. B. and Hurrell, M. R. (1985). "Settlement development caused by tunnelling in soil." *Ground Engineering*, Vol. 18, No. 8, pp. 17-20.

Attewell, P. B. and Woodman, J. P. (1982). "Predicting the dynamics of ground settlement and its derivitives caused by tunnelling in soil." *Ground Engineering*, Vol. 15, No. 8, pp. 13-22,36.

Bolton, M. D., Lu, Y. C., and Sharma, J. S. (1996). "Centrifuge models of tunnel construction and compensation grouting." *Int. Symp. on Geotech. Aspects of Underground Constr. in Soft Ground. Balkema, Rotterdam*, pp. 471-477.

Celestino, T. B., Gomes, R. A. M. P., and Bortolucci, A. A. (2000). "Errors in ground distortions due to settlement trough adjustment." *Tunnelling and Underground Space Technology*, Vol. 15, No. 1, pp. 97-100, DOI: 10.1016/S0886-7798(99)00054-1.

Chakeri, H., Ozcelik, Y., and Unver, B. (2013). "Effects of important factors on surface settlement prediction for metro tunnel excavated by EPB." *Tunnelling and Underground Space Technology*, Vol. 36, pp. 14-23, DOI: 10.1016/j.tust.2013.02.002.

Chapman, D. N., Ahn, S. K., and Hunt, D. V. L. (2007). "Investigating ground movements caused by the construction of multiple tunnels in soft ground using laboratory model tests." *Canadian Geotechnical Journal*, Vol. 44, No. 6, pp. 631-643, DOI: 10.1139/t07-018.

Chen, R. P., Zhu, J., Liu, W., and Tang, X. W. (2011). "Ground movement induced by parallel EPB tunnels in silty soils." *Tunnelling and Underground Space Technology*, Vol. 26, No. 1, pp. 163-171, DOI: 10.1016/j.tust.2010.09.004.

Chou, W.-I. and Bobet, A. (2002). "Predictions of ground deformations in shallow tunnels in clay." *Tunnelling and Underground Space Technology*, Vol. 17, No. 1, pp. 3-19, DOI: 10.1016/S0886-7798 (01)00068-2.

Fang, Y., Yang, Z., Cui, G., and He, C. (2015). "Prediction of surface settlement process based on model shield tunnel driving test." *Arabian Journal of Geoscience*, Vol. 8, pp. 7787-7796, DOI: 10.1007/s12517-015-1800-0.

Franzius, J. N., Potts, D. M., and Burland, J. B. (2005). "The influence of soil anisotropy and K0 on ground surface movements resulting from tunnel excavation." *Géotechnique,* Vol. 55, No. 3, pp. 189-199, DOI: 10.1680/geot.2005.55.3.189.

Gharahbagh, E. A., Rostami, J., and Talebi, K. (2014). "Experimental study of the effect of conditioning on abrasive wear and torque requirement of full face tunneling machines." *Tunnelling and Underground Space Technology*, Vol. 41, pp. 127-136, DOI: 10.1016/j.tust.2013.12.003.

Grasmick, J., Mooney, M., Rysdahl, B., Prantil, E., and Thompson, A. (2015). "Evaluation of slurry TBM design support pressures using east side access queens bored tunnels data." *Proc. Rapid Excavation and Tunneling Conference*, New Orleans, LA, June, pp. 7-10.

He, C., Feng, K., Fang, Y., and Jiang, Y. C. (2012). "Surface settlement caused by twin-parallel shield tunnelling in sandy cobble strata." *Journal of Zhejiang University SCIENCE A,* Vol. 13, No. 11, pp. 858-869, DOI: 10.1631/jzus.A12ISGT6.

Kim, S.-H. (1996). *Model testing and analysis of interactions between tunnels in clay*, University of Oxford.

Lee, K. M., Ji, H. W., Shen, C. K., Liu, J. H., and Bai, T. H. (1999). "Ground response to the construction of shanghai metro tunnel-Line 2." *Soils and Foundations*, Vol. 39, No. 3, pp. 113-134.

Lee, K. and Rowe, R. (1991). "An analysis of three-dimensional ground movements: The thunder bay tunnel." *Canadian Geotechnical Journal,* Vol. 28, No. 1, pp. 25-41.

Liao, S. M., Liu, J. H., Wang, R. L., and Li, Z. M. (2009). "Shield tunneling and environment protection in Shanghai soft ground." *Tunnelling and underground space technology,* Vol. 24, No. 4, pp. 454-465, DOI: 10.1016/j.tust.2008. 12.005.

Liu, J. H. and Hou, X. Y. (1991). *Shield method tunnel*, China Railway Press, Beijing (in Chinese).

Loganathan, N., Poulos, H. G., and Stewart, D.P. (2000). "Centrifuge model testing of tunnelling-induced ground and pile deformations." *Géotechnique*, Vol. 50, No. 3, pp. 283-294, DOI: 10.1680/geot. 2000.50.3.283.

Mair, R. J., Taylor, R. N., and Bracegirdle, A. (1993). "Subsurface settlement profiles above tunnels in clays." *Géotechnique*, Vol. 43, No. 2, pp. 315-320.

Marshall, A. M., Farrell, R., Klar, A., and Mair, R. (2012). "Tunnels in sands: The effect of size, depth and volume loss on greenfield displacements." *Géotechnique*, Vol. 62, No. 5, pp. 385-399, DOI: 10.1680/geot.10.P.047.

Marshall, A. M. and Mair, R. J. (2011). "Tunneling beneath driven or jacked end-bearing piles in sand." *Canadian Geotechnical Journal,* Vol. 48, No. 12, pp. 1757-1771, DOI: 10.1139/t11-067.

Mathew, G. V. and Lehane, B. M. (2012). "Numerical back-analyses of greenfield settlement during tunnel boring." *Canadian Geotechnical Journal*, Vol. 50, No. 2, pp. 145-152, DOI: 10.1139/cgj-2011-0358.

Melis, M., Medina, L., and Rodriguez, J. M. (2002). "Prediction and analysis of subsidence induced by shield tunnelling in the Madrid Metro extension." *Canadian Geotechnical Journal,* Vol. 39, No. 6, pp. 1273-1287, DOI: 10.1139/t02-073.

Merritt, A. and Mair, R. J. (2006). "Mechanics of tunnelling machine screw conveyors: Model tests." *Géotechnique*, Vol. 56, No. 9, pp. 605-615, DOI: 10.1680/geot.2006.56.9.605.

Merritt, A. and Mair, R. J. (2008). "Mechanics of tunnelling machine screw conveyors: A theoretical model." *Géotechnique*, Vol. 58, No. 2, pp. 79-94, DOI: 10.1680/geot.2008.58.2.79.

Mooney, M., Grasmick, J., Kenneally, B., and Fang, Y. (2015). "The role of slurry TBM parameters on ground deformation: field results and computational modeling." *Proc. Intl. Conf. on Tunnel Boring Machines in Difficult Grounds (TBM DiGs)*, Singapore, November, pp. 18-20.

Nazem, A., Hossaini, M. F., Rahami, H., and Bolghonabadi, R. (2015). "Optimization of conformal mapping functions used in developing

closed-form solutions for underground structures with conventional cross sections." *Int. Journal of Mining & Geo-Engineering*, Vol. 49, No. 1, pp. 93-102.

Nomoto, T., Imamura, S., Hagiwara, T., Kusakabe, O., and Fujii, N. (1999). "Shield tunnel construction in centrifuge." *Journal of Geotechnical and Geoenvironmental Engineering,* Vol. 125, No. 4, pp. 289-300, DOI: 10.1061/(ASCE)1090-0241(1999) 125:4(289).

O'reilly, M. and New, B. (1982). "Settlements above tunnels in the United Kingdom-their magnitude and prediction." *Proc. Tunnelling 82, Institution of Mining and Metallurgy*, London, pp. 173-181.

Papastamos, G., Stiros, S., Saltogianni, V., and Kontogianni, V. (2014). "3-D strong tilting observed in tall, isolated brick chimneys during the excavation of the Athens Metro." *Applied Geomatics*, Vol. 7, No. 2, pp. 115-121.

Park, K.-H. (2005). "Analytical solution for tunnelling-induced ground movement in clays." Tunnelling and Underground Space Technology, Vol. 20, No. 3, pp. 249-261, DOI: 10.1016/j.tust.2004.08.009.

Park, K. (2004). "Elastic solution for tunneling-induced ground movements in clays." *International Journal of Geomechanics,* Vol. 4, No. 4, pp. 310-318, DOI: 10.1061/(ASCE)1532-3641(2004)4:4(310).

Peck, R. B. (1969). "Deep excavations and tunnelling in soft ground." *Proc. 7th Int. Conf. on Soil Mechanics and Foundation Engineering,* Mexico, pp. 225-290.

Peila, D., Oggeri, C., and Vinai, R. (2007). "Screw conveyor device for laboratory tests on conditioned soil for EPB tunneling operations." *Journal of Geotechnical and Geoenvironmental Engineering,* Vol. 133, No. 12, pp. 1622-1625, DOI: 10.1061/(ASCE)1090-0241 (2007)133:12(1622).

Peila, D. Picchio, A., and Chieregato, A. (2013). "Earth pressure balance tunnelling in rock masses: Laboratory feasibility study of the conditioning process." *Tunnelling and Underground Space Technology,* Vol. 35, pp. 55-66, DOI: 10.1016/j.tust.2012.11.006.

Sagaseta, C. (1987). "Analysis of undraind soil deformation due to ground loss." *Discussion: Géotechnique*, Vol. 37, No. 3, pp. 301-320.

Sagaseta, C. (1988). "Analysis of undrained soil deformation due to ground loss." *Géotechnique*, Vol. 38, No. 4, pp. 647-649.

Schmidt, B. (1969). "A method of estimating surface settlement above tunnels constructed in soft ground." *Can Geotech J*, Vol. 20, pp. 11-22.

Sugiyama, T., Hagiwara, T., Nomoto, T., Nomoto, M., Ano, Y., and Mair, R. J. (1999). "Observations of ground movements during tunnel construction by slurry shield method at the Docklands Light Railway Lewisham extension east London." *Soils and Foundations*, Vol. 39, No. 3, pp. 99-112.

Teng, L. and Zhang H. (2012). "Meso-Macro analysis of surface settlement characteristics during shield tunneling in sandy cobble ground." *Rock and Soil Mechanics*, Vol. 33, No. 4, pp. 1141-1150. (In Chinese)

Verruijt, A. and Booker, J. (1996). "Surface settlements due to deformation of a tunnel in an elastic half plane." *Géotechnique*, Vol. 46, pp. 753-756, DOI: 10.1680/geot.1998.48.5.709.

Vinai, R., Oggeri, C., and Peila, D. (2008). "Soil conditioning of sand for EPB applications: A laboratory research." *Tunnelling and Underground Space Technology*, Vol. 23, No. 3, pp. 308-317, DOI: 10.1016/j.tust.2007.04.010.

Vorster, T. E., Klar, A., Soga, K., and Mair, R. J. (2005). "Estimating the effects of tunneling on existing pipelines." *Journal of Geotechnical and Geoenvironmental Engineering*, Vol. 131, No. 11, pp. 1399-1410, DOI: 10.1061/(ASCE)1090-0241(2005)131:11(1399).

Zhu, H. H., Xu, Q. W., Liao, S. M., Fu, D. M., and Yu, N. (2006). "Experimental study on working parameters of EPB shield machine." *Yantu Gongcheng Xuebao (Chinese Journal of Geotechnical Engineering)*, Vol. 28, No. 5, pp. 553-557. (In Chinese)